

## Tailoring Band Gap and Hardness by Intercalation: An *ab initio* Study of $I_8@Si-46$ and Related Doped Clathrates

D. Connétable,<sup>1</sup> V. Timoshevskii,<sup>1</sup> E. Artacho,<sup>2</sup> and X. Blase<sup>1</sup>

<sup>1</sup>Département de Physique des Matériaux and CNRS, Université Claude Bernard-Lyon 1, Bâtiment 203, 43 Bd du 11, Novembre 1918, 69622 Villeurbanne Cédex, France

<sup>2</sup>Department of Earth Sciences, University of Cambridge, Downing Street, Cambridge CB2 3EQ, United Kingdom

(Received 14 May 2001; published 29 October 2001)

We present an *ab initio* study of the structural and electronic properties of the recently synthesized  $I_8@Si-46$  clathrate which is shown to be a degenerate *p*-type doped system. The intercalation significantly opens the band gap to a 1.75 eV value within the density functional theory. We study further the intercalation by other neighboring elements. A quasiparticle study reveals that such systems can display a band gap in the “green-light” energy range. Finally, we show that the bulk modulus can be increased to values equivalent to the one of the diamond phase.

DOI: 10.1103/PhysRevLett.87.206405

PACS numbers: 71.20.Tx, 62.20.-x, 81.05.Zx, 82.75.-z

The increasing integration of electronic devices puts a strong emphasis on trying to design semiconducting compounds which are compatible with the silicon-based technology available today. In particular, materials displaying a large band gap in the optical range, for use in optoelectronic devices, certainly do exist but they are not based on silicon, putting strong constraints on an all-integrated fabrication technology. Several routes have been recently proposed [1,2], but it is difficult at this stage to conclude on their effective applicability.

A promising silicon phase has recently attracted much attention for its specific structural and electronic properties. Silicon clathrates [3] are cage-like materials composed of face-sharing  $Si_{20}$ ,  $Si_{24}$ , and  $Si_{28}$  clusters. The discovery of the up to  $\sim 8$  K superconductivity of doped clathrates [4], the prediction [5–10] confirmed by experiment [11] that the band gap of Si clathrates is  $\sim 0.7$  eV larger than the one of Si diamond, the low compressibility of such phases [12], and the high thermoelectric power of doped clathrates [13] have generated much work at the experimental and theoretical level.

Intercalation, or doping, of clathrates can be achieved by filling up the cages by individual atoms (Fig. 1). So far, much attention has been paid to Ba- and Na-doped clathrates [6–8,10]. More recently, the synthesis of iodine doped Si-46 clathrates [14] has been achieved, and its structural properties under pressure have been explored [15]. This is the first Si clathrate doped with an element more electronegative than the host network.

In this Letter, we present first-principles calculations of the structural and electronic properties of  $I_8@Si-46$  clathrates. Contrary to Ba- and Na-doped clathrates [6,7], we show that strong hybridizations between the iodine and Si network orbitals result in a large opening of the band gap. This is shown to stem from a preferential coupling with the bottom of the conduction bands due to symmetry arguments. Identical results are obtained for  $Xe_8@Si-46$  for which we perform an accurate quasiparticle calcu-

lation predicting a 2.25 eV visible-light band gap, thus opening new perspectives for all integrated silicon-based technologies. We show further that it is also possible to increase the bulk modulus of clathrates to values equivalent to the one of the Si-2 phase by a proper choice of the intercalated atom.

Our calculations are mainly performed within the local density approximation (LDA) to the density functional theory (DFT) [16] besides a quasiparticle calculation of the band structure of  $Xe_8@Si-46$ . A pseudopotential approach is used [17] with a plane-wave expansion of the wave functions. Scalar relativistic effects are included at the pseudopotential level and core correction is used [18]. A 16 Ry cutoff is imposed except for the calculations of the cohesive energy at the equilibrium volume for which it is increased up to 20 Ry. The Brillouin zone is sampled by

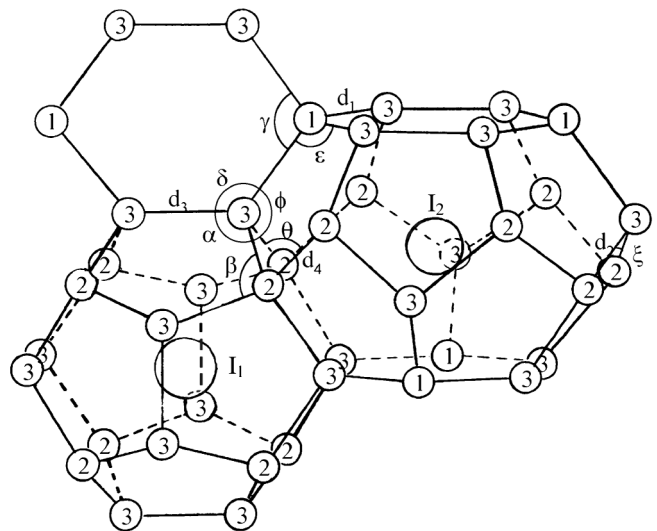


FIG. 1. Symbolic ball-and-stick representation of  $I_8@Si-46$  clathrates. The nonequivalent Si atoms, distances, and angles are labeled differently.

TABLE I. Calculated bulk modulus (GPa), binding energy (eV), and lattice parameter  $a_0$ (Å) for  $M_8$ @Si-46 clathrates. A negative binding energy means that the  $M$  element is not binding inside the cages. The bulk modulus of Si-2 is calculated to be 97 GPa.

$M$ element	Si-46	Sn	Te	I	Xe
$B_0^{\text{theo}}$	87	97	95	91	85
$E^{\text{bonding}}$	...	3.3	3.1	1.7	-0.6
$a_0$	10.05	10.04	10.06	10.13	10.23

a  $2 \times 2 \times 2$  grid [19]. For the calculation of the density of states, the sampling is refined to a  $8 \times 8 \times 8$  grid. The use of such increased cutoffs allows one to check for the good convergency of our calculations.

We first study the  $I_8$ @Si-46 compound which crystallizes in the type I clathrate structure made of  $Si_{20}$  and  $Si_{24}$  clusters. Each cage is filled by one iodine atom (Fig. 1). A structural relaxation was performed at several unit cell volumes and the calculated points were fit by a Murnaghan equation of states. The equilibrium lattice parameter of  $I_8$ @Si-46 is found to be 10.13 Å, which is  $\sim 0.8\%$  larger than the one of Si-46. The cohesive energy of iodine inside the clathrate network, taking as a reference the energy of the undoped Si-46 clathrate and the isolated iodine atom, is calculated to be 1.7 eV/atom (see Table I). Further, taking for the iodine atom reference energy its energy in the  $I_2$  molecule, we find that iodine prefers to sit inside the clathrate cages by 0.65 eV/atom.

We plot in Fig. 2 the LDA band structure of  $I_8$ @Si-46 along high-symmetry directions of the Brillouin zone. Because of the electronegativity of iodine, the Fermi level  $E_F$  is located 0.26 eV below the energy gap.  $I_8$ @Si-46 is therefore a  $p$ -type doped semiconductor. The comparison of the  $I_8$ @Si-46 and Si-46 band structures clearly shows that the “rigid-band model,” consisting of a shift under doping of the Fermi level without modification of the host network band structure, is not appropriate for the present system, in great contrast with the case of  $Ba_xNa_{8-x}$ @Si-46 compounds. In particular, we find that

the band gap is increased from 1.2 to 1.75 eV under doping (DFT value).

The case of  $Xe_8$ @Si-46, which displays a 1.65 eV band gap, reveals that ionic effects are not at the origin of such a band gap opening. From the comparison of the band structure of Si-46 and  $Xe_8$ @Si-46 (Fig. 2), we find that the top of the valence bands is only slightly modified upon introduction of the Xe atoms, while the bottom of the conduction bands changes dramatically as in  $I_8$ @Si-46. This indicates that the coupling between the Xe (or I) orbitals take place mainly with the bottom of the conduction bands, thus opening the band gap by repulsion. The analysis of the symmetry character of the Si-46 states at  $\Gamma$  ( $O_h$  group) shows that the top of the valence and bottom of the conduction bands belong, respectively, to the  $A_{1u}$  and  $T_{1u}$  representations. The set of representations into which the Xe or I orbitals split in the  $O_h$  crystal field includes  $T_{1u}$  but not  $A_{1u}$  so that indeed only the bottom of the conduction bands can couple to the intercalated atom orbitals.

There exists, of course, states below the top of the valence band which can interact with the Xe orbitals. In particular, the two closest bands (of  $E_u$  and  $T_{2g}$  character at  $\Gamma$ ) are pushed up in energy but the repulsion is not large enough for them to enter the band gap (see Fig. 2). It is interesting to note as well that similar effects can be observed in the case of Xe and I doped  $Si_{20}H_{20}$  and  $Si_{24}H_{24}$  clusters for which, as in the crystal, we find that the band gap opens by repulsion with the lowest unoccupied orbitals while symmetry forbids the coupling with the highest occupied states located within  $\sim 1$  eV of the bottom of the band gap.

Further information can be obtained from the electronic density of states (eDOS) projected onto the atomic orbitals. We use the SIESTA package which is a self-consistent DFT-LDA pseudopotential code based on atomiclike numerical orbitals [20]. In the case of  $Xe_8$ @Si-46, there is hardly any Xe weight at the top of the valence bands and the Xe- $5p$  states lie in the middle of the valence bands. In the case of  $I_8$ @Si-46 (Fig. 3), charge transfer brings the highest occupied I states to the Fermi level. The similarity between the band structures of  $Xe_8$ @Si-46 and  $I_8$ @Si-46

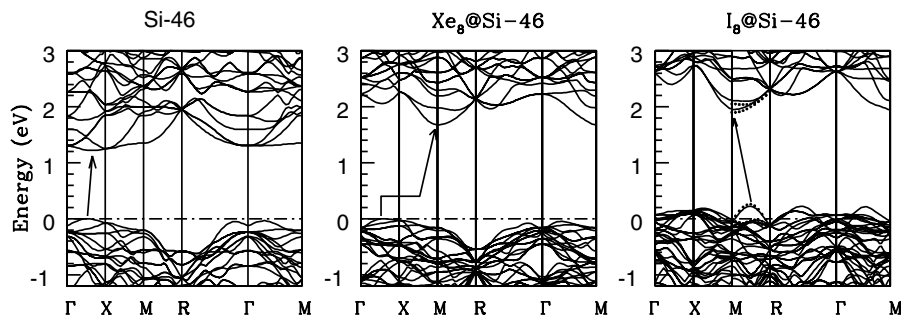


FIG. 2. DFT-LDA band structure of (left) Si-46, (center)  $Xe_8$ @Si-46, and (right)  $I_8$ @Si-46 along high-symmetry directions of the Brillouin zone. Energies are in eV. The zero of energy has been set to the top of the valence bands for Si-46 and  $Xe_8$ @Si-46 and to the Fermi level for  $I_8$ @Si-46. The dots indicate the all-electron calculation values (see Ref. [18]). The arrows indicate the nature of the gap.

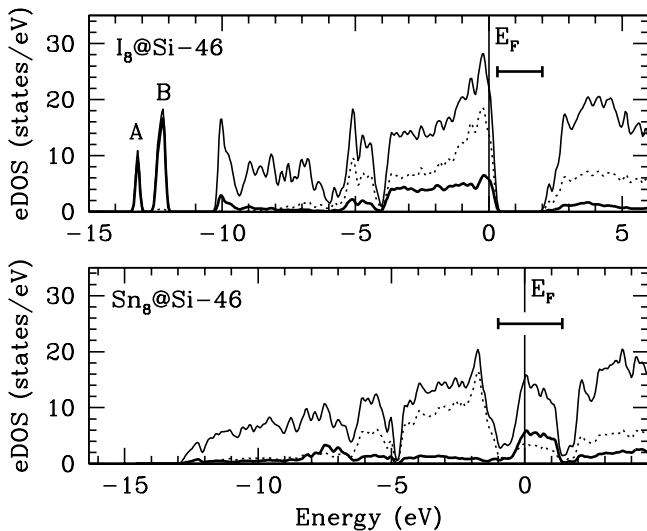


FIG. 3. Plot of the electronic density of states (eDOS) for  $I_8@Si-46$  and  $Sn_8@Si-46$ . The thin and thick lines correspond, respectively, to the total eDOS and to the eDOS projected on the dopant atom orbitals. The dotted lines are the Si-3p projected eDOS. The horizontal bracketed sections of line indicate the “band gap” (in the case of  $Sn_8@Si-46$ , it just refers to the observed depletion in Si weight). For sake of comparison, the low-energy bound of these band gaps have been aligned in the upper and lower eDOS. A 0.1 eV broadening has been used.

at the bottom of the conduction bands indicates that besides this charge transfer effect, hybridizations are similar in both compounds. The integrated eDOS shows that there are exactly four states between  $E_F$  and the bottom of the gap, corresponding to the eight electrons missing in the unit cell on the I-5p shells. The I-5s orbitals are found to lie at much lower energy. The splitting of these orbitals (peaks A and B) reveals that as expected the iodine atoms in the smallest  $Si_{20}$  cages interact more strongly with the silicon orbitals.

The DFT-LDA approach is well-known to underestimate the band gap of semiconducting systems. In particular, the DFT-LDA band gap of Si-2 and Si-34 are too small by  $\sim 0.7$  eV as compared to experiment. We have therefore performed for  $Xe_8@Si-46$  a quasiparticle calculation within the GW approximation. Such an approach is known to yield electronic excitation energies within a  $\sim 0.1$  eV accuracy as compared to experimental results for this type of system [21]. The quasiparticle correction was calculated at  $\Gamma$ ,  $M$ , and  $X$ . The results are quoted in Table II showing that the DFT band gap is opened by  $\sim 0.6$  eV by the GW correction, yielding a  $\sim 2.25$  eV band gap, that is, a silicon based “green light” semiconductor system. Such a result confirms the DFT prediction that *doped clathrates may be potentially important in the making of silicon-based optoelectronic devices*.

We finally complete our study of  $M_8@Si-46$  doped clathrates by studying the evolution of the structural and electronic properties going from  $M = I$  to  $M = Sn$ . The reduction of the electronegativity of the elements going

TABLE II. Calculated LDA and GW top of the valence bands (index  $v$ ) and bottom of the conduction bands (index  $c$ ) at the  $\Gamma$ ,  $X$ , and  $M$  points. The zero of energy is taken to be the highest occupied state at  $X$  (located  $\sim 15$  meV below the top of the valence bands within LDA).

	$\Gamma_v$	$\Gamma_c$	$X_v$	$X_c$	$M_v$	$M_c$
LDA	-0.12	2.25	0.00	2.27	-0.14	1.66
GW	-0.13	2.87	0.00	2.90	-0.15	2.26

to the left of the periodic table suggests that the bonding between intercalated and silicon atoms should become less ionic and more covalent. The most striking trends are the reduction of the volume cell size to values lower than the one of Si-46 and the strong increase of the bulk modulus  $B_0$ . We emphasize, in particular, that while the atomic radius increases from Xe to Sn, the volume of the corresponding intercalated clathrate decreases. While the bulk modulus of  $Xe_8@Si-46$  collapses to 85 GPa (that is, 2.3% lower than the empty phase), the bulk modulus of  $I_8@Si-46$  is found to be already 4.6% larger. Further, intercalating by elements less electronegative than iodine increases significantly  $B_0$  up to 97 GPa in the case of Sn, that is, a value which within the error bar [22] is equivalent to the  $B_0$  of the Si-2 diamond phase. This can be related to a more covalent character of the bonds between the intercalated atom and the Si network.

It is surprising that materials with stretched Si-Si bonds and which are metallic may exhibit a bulk modulus equivalent to the one of the diamond phase (see Ref. [23]). In particular, as shown in Fig. 3,  $Sn_8@Si-46$  is a true metal with a large eDOS at the Fermi level. To rationalize these results, we note that the interaction between Si and the intercalated atoms means that its effective coordination is larger than four. As such, doped clathrates can be regarded as highly coordinated phases of Si (meta)stable at ambient pressure, providing an explanation for the decrease of the compressibility.

In conclusion, we have studied the structural and electronic properties of  $M_8@Si-46$  doped clathrates, where  $M = I$  and other neighboring elements of the periodic table. We have shown on the basis of quasiparticle GW calculations that the band gap of such compounds can be as large as  $\sim 2.25$  eV, thus providing much perspective in the use of such phases in optoelectronic applications. We have evidenced further that under intercalation the bulk modulus can be increased significantly to values equivalent to the one of the diamond Si-2 phase. This result offers a new path towards the synthesis of ultrahard materials and invites one to study carbon-based clathrates.

The authors acknowledge use of the supercomputer facilities at the French CNRS (IDRIS, Orsay) and at the *Commissariat à l’Energie Atomique* (CEA-CENG) in Grenoble, France. V.T. is supported by the Région Rhones-Alpes. E.A. acknowledges support of the Spanish Ministerio de Ciencia y Tecnología under Grant

No. BFM-2000-1312. X. B. is indebted to P. Mélinon for useful discussions and to E. Reny for providing Fig. 1 from his Ph.D. thesis.

*Note added.*—Similar band gap modifications under doping have been recently predicted theoretically for free clusters. See, Hiura, Miyazaki, and Kanayama [24]; Kumar and Kawazoe [25].

- 
- [1] Wait Lek NG, M. A. Lourenço, R. M. G. William, S. Ledain, G. Shao, and K. P. Homewood, *Nature (London)* **410**, 192 (2001).
- [2] P. Zhang, V. H. Crespi, E. Chang, S. G. Louie, and M. L. Cohen, *Nature (London)* **409**, 69 (2001).
- [3] J. Kasper, P. Hagemuller, M. Pouchard, and C. Cros, *Science* **150**, 1713 (1965).
- [4] H. Kawaji, H. Horie, S. Yamanaka, and M. Ishikawa, *Phys. Rev. Lett.* **74**, 1427 (1995); J. D. Bryan, V. I. Srdanov, G. D. Stucky, and D. Schmidt, *Phys. Rev. B* **60**, 3064 (1999); S. Yamanaka, E. Enishi, H. Fukuoka, and M. Yasukawa, *Inorg. Chem.* **39**, 56–58 (2000).
- [5] G. B. Adams, M. O’Keeffe, A. A. Demkov, O. F. Sankey, and Y.-M. Huang, *Phys. Rev. B* **49**, 8048 (1994).
- [6] A. A. Demkov *et al.*, *Phys. Rev. B* **50**, 17001 (1994).
- [7] S. Saito and A. Oshiyama, *Phys. Rev. B* **51**, 2628 (1995).
- [8] V. I. Smelyanski and J. S. Tse, *Chem. Phys. Lett.* **264**, 459 (1997).
- [9] P. Mélinon *et al.*, *Phys. Rev. B* **58**, 12 590 (1998).
- [10] K. Moriguchi, S. Munetoh, and A. Shintani, *Phys. Rev. B* **62**, 7138 (2000); K. Moriguchi, M. Yonemura, A. Shintani, and S. Yamanaka, *Phys. Rev. B* **61**, 9859 (2000).
- [11] J. Gryco *et al.*, *Phys. Rev. B* **62**, R7707 (2000).
- [12] A. San-Miguel *et al.*, *Phys. Rev. Lett.* **83**, 5290 (1999).
- [13] J. L. Cohn *et al.*, *Phys. Rev. Lett.* **82**, 779 (1999); J. S. Tse *et al.*, *Phys. Rev. Lett.* **85**, 114 (2000).
- [14] E. Reny, S. Yamanaka, C. Cros, and M. Pouchard, *Chem. Commun.* **24**, 2505 (2000). In their work, Reny *et al.* proposed a  $I_8@Si_{46-x}I_x$  ( $x \sim 1.8$ ) stoichiometry with  $x$  iodine atoms in substitution. We focus here on the “ideal”  $I_8@Si$ -46 structure and await further experimental characterizations of the structure of iodine doped clathrates.
- [15] A. San Miguel *et al.* (to be published).
- [16] P. Hohenberg and W. Kohn, *Phys. Rev.* **136**, B864 (1964); W. Kohn and L. J. Sham, *Phys. Rev.* **140**, A1133 (1965); D. M. Ceperley and B. J. Alder, *Phys. Rev. Lett.* **45**, 566 (1980).
- [17] N. Troullier and J. L. Martins, *Phys. Rev. B* **43**, 1993 (1991); K. Kleinman and D. M. Bylander, *Phys. Rev. Lett.* **48**, 1425 (1982).
- [18] An all-electron calculation was performed using the FLAPW WIEN97 package. See P. Blaha, K. Schwarz, and J. Luitz, Technical University of Vienna, Austria, (ISBN 3-9501031-0-4). Scalar-relativistic effects were included in the muffin-tin spheres. We have studied the MR direction for the  $I_8@Si$ -46 compound. Aligning the Fermi levels, we find that around the gap the all-electron and pseudopotential calculations agree within better than 0.1 eV (see Fig. 2).
- [19] H. J. Monkhorst and J. D. Pack, *Phys. Rev. B* **13**, 5188 (1976).
- [20] A well-converged DZP basis (doubled  $\{s, p_x, p_y, p_z\}$  orbitals plus  $d$ -polarization orbitals) has been used. We have verified that within this NAO DZP basis adopted, both the structural and electronic properties of  $I_8@Si$ -46 are in excellent agreement with the plane-wave basis results. See P. Ordejón, E. Artacho, and J. M. Soler, *Phys. Rev. B* **53**, R10 441 (1996); D. Sánchez-Portal, P. Ordejón, E. Artacho, and J. M. Soler, *Int. J. Quantum Chem.* **85**, 453 (1997).
- [21] M. Hybertsen and S. G. Louie, *Phys. Rev. B* **34**, 5390 (1985), and references therein. In the present work, a 3 a.u.  $G_{\max}$  cutoff and up to 800 conduction bands were used in the construction of the dielectric matrix and self-energy operator. More technical details will be given elsewhere [X. Blase (to be published)].
- [22] We have verified that the scaling-law correction proposed by Rignanese *et al.* [*Phys. Rev. B* **52**, 8160 (1995)] to correct for the basis-size variation with volume did not affect significantly our calculated value. This effect together with the variation of the bulk modulus with the choice of the fitted data points can be estimated to yield an error of less than  $\pm 1$  GPa.
- [23] A. Liu and M. Cohen, *Science* **245**, 841 (1989).
- [24] H. Hiura, T. Miyazaki, and T. Kanayama, *Phys. Rev. Lett.* **86**, 1733 (2001).
- [25] V. Kumar and Y. Kawazoe, *Phys. Rev. Lett* **87**, 045503 (2001).